Exploiting Interference in Joint Radar-Communication Transmission

Jianjun Zhang
College of Computer Science and Technology
Nanjing University of Aeronautics and Astronautics
Nanjing, China
jianjun.zhang@nuaa.edu.cn

Fan Liu
Department of Electronic and Electrical Engineering
Southern University of Science and Technology
Shenzhen, China
liuf6@sustech.edu.cn

Christos Masouros
Department of Electronic & Electrical Engineering
University College London
London, U.K.
c.masouros@ucl.ac.uk

Yongming Huang
National Mobile Communications Research Laboratory
Southeast University
Nanjing, China
huangym@seu. edu.cn

***Abstract*—By sharing the same hardware platform, spectral resource as well as transmit waveform, dual-functional radar-communication (DFRC) based integrated sensing and communication (ISAC) framework has been envisioned as a key technology for future wireless networks. Most DFRC beamforming works focus on block-level precoding, which fails to exploit constructive interference. To tackle this issue, we propose symbol-level joint radar sensing and communication beamforming algorithms in this paper. First, we formulate the problem of joint radar-communication beamforming based on symbol-level precoding (SLP) by incorporating constructive interference into SLP, so as to improve the energy efficiency. To address the formulated problem, we tailor a highly parallelizable iterative algorithm, which is shown to converge to stationary points. To achieve better performance, we further propose an efficient recursive optimization algorithm. In particular, the recursive algorithm monotonously improves the performance of interest as the recursive procedure proceeds.**

***Index Terms*—Integrated sensing and communication, symbol-level precoding, parallel optimization, recursive design.**

I. Introduction

The integrated sensing and communication (ISAC) technology has attracted considerable attention recently, because it can improve spectral and/or energy efficiency, reduce hardware cost and power consumption [1], [2]. The current DFRC systems can be classified into three categories, i.e., the radar-centric designs [3]–[5], communication-centric designs [6]–[8] and joint designs [9]–[11]. For the first category, information signalling is modulated in a known radar waveform. Although performance loss in terms of radar sensing is negligible, since the radar signalling remains largely unchanged, the data rate is very limited. For the communication-centric mode, the design priority focuses on communication, and thus the radar sensing is a secondary function added on to a communication system. The main approach is to exploit communication waveform to extract radar information through target echoes. For this design mode, a possible drawback is that the sensing performance is scenario-dependent and difficult-to-tune.

Compared with the first two categories, the joint design or optimization mode is the most flexible, which can facilitate to balance different design requirements from communication and sensing and often offers a better trade-off between the two functions. Among various research problems, joint waveform optimization (WO) is pivotal to pursue a desired performance tradeoff by adopting appropriate performance metrics [9]. Most desired waveforms can be obtained by optimizing spatial precoders, e.g., waveform (or beam-pattern) similarity based WO [9], [10] or mutual information based WO [12], [13]. In contrast to most communication-only precoding or beamforming designs, space-time processing is indispensable for an ISAC task, so as to accomplish the radar sensing task.

It is well-known that one of the most primary motivations of ISAC is to improve the energy efficiency [14]. However, for most DFRC designs, the block-level precoding scheme is chosen to optimize a communication performance metric, which fails to fully exploit multi-user interference. An efficient scheme to exploit multi-user interference is symbol-level precoding (SLP) [15], where the interference is exploited from an instantaneous point of view. In particular, the concept of constructive interference (CI) was exploited in [16]–[19] to improve system performance. Notably, as the first work on optimization based CI precoding, a low-complexity vector precoding scheme was proposed in [16] for the limited feedback downlink multi-user multi-input single-output (MISO) system. Despite the advantages of SLP above, only very limited works have incorporated SLP into DFRC designs [20], [21]. Besides, the high computational complexity is seldom considered.

In this paper, we propose efficient symbol-level joint radar sensing and communication beamforming algorithms. First, to exploit the multi-user interference and thus improve the energy efficiency of the DFRC system, we formulate the problem of joint radar-communication beamforming optimization based on SLP and, particularly, incorporate the CI constraints into the problem of interest. To address the formulated non-convex problem, we propose an efficient parallelizable iterative algorithm, which can exploit latent separability of the optimization problem. We also show that the iterative algorithm converges to the stationary points. To exploit the space-time processing feature, we propose a recursive design idea for the SLP-based DFRC beamforming problem, and further propose an efficient recursive algorithm and reveal useful insights. In particular, we show that the recursive algorithm can monotonously improve the performance as the recursive procedure proceeds.

II. System Model

Consider a MIMO DFRC base station (BS) equipped with $N_{\rm T}$ transmit antennas and $N_{\rm R}$ receive antennas. To avoid information loss of sensed targets for a radar task, it is often required $N_{\rm T} < N_{\rm R}$. Meanwhile, the BS serves U single-antenna users (UEs), denoted by $\mathcal{U} = \{1, \cdots, U\}$. The channel vector between the BS and each UE $u \in \mathcal{U}$ is denoted by $\mathbf{h}_u \in \mathbb{C}^{N_{\rm T}\times 1}$. Let $\mathbf{X} \in \mathbb{C}^{N_{\rm T}\times L}$ be a DFRC signal matrix, where L is the length of radar pulse or communication frame. The matrix $\mathbf{X}$ has dual identities. On the one hand, from the perspective of communication, x_{ij} (i.e., the (i,j)-th entry of $\mathbf{X}$) represents the discrete signal sample transmitted at antenna i and time-slot j. On the other hand, from the view of radar, x_{ij} is the j-th fast-time snapshot transmitted at antenna i.

When $\mathbf{X}$ is transmitted by the BS, the signals received by the U UEs can be compactly written by

$$\mathbf{Y}_{\rm C} = \mathbf{H}\mathbf{X} + \mathbf{Z}_{\rm C}, \tag{1}$$

where $\mathbf{Z}_{\rm C} \in \mathbb{C}^{U\times L}$ is the received noise matrix with each column distributed as $\mathcal{CN}(\mathbf{0}, \sigma_{\rm C}^2\mathbf{I})$, and $\mathbf{H} = [\mathbf{h}_1, \mathbf{h}_2, \cdots, \mathbf{h}_U]^{\rm H}$ collects all channel vectors of the UEs. Note that the transmitted matrix $\mathbf{X}$ is a nonlinear function of transmitted information symbols, i.e., $\mathbf{X} = \mathbf{X}(\mathbf{S})$, where $\mathbf{S} = [\mathbf{s}_1, \mathbf{s}_2, \cdots, \mathbf{s}_L] \in \mathbb{C}^{U\times L}$ collects intended information symbols.

When $\mathbf{X}$ is transmitted to sense a target, the reflected echo signal matrix at the receiver of the BS can be written as

$$\mathbf{Y}_{\rm R} = \mathbf{G}\mathbf{X} + \mathbf{Z}_{\rm R}, \tag{2}$$

where, similarly, $\mathbf{Z}_{\rm R}$ denotes the received noise matrix with each column distributed as $\mathcal{CN}(\mathbf{0}, \sigma_{\rm R}^2\mathbf{I})$. $\mathbf{G} \in \mathbb{C}^{N_{\rm R}\times N_{\rm T}}$ in (2) denotes the target response matrix and can be expressed as

$$\mathbf{G} = \sum_{i=1}^{V} \alpha_i \mathbf{b}(\theta_i)\mathbf{a}^{\rm H}(\theta_i), \tag{3}$$

where $\mathbf{b}(\cdot)$ and $\mathbf{a}(\cdot)$ denote the array response vectors.

Without loss of generality, the PSK modulation mode (with constellation $\mathcal{D}$ of size D) is considered in this paper. Nevertheless the developed algorithms can be trivially extended to other modulation modes. The (u,l)-th element of $\mathbf{S}$ is denoted by $s_{u,l}$. Let $s_{u,l} = e^{j\xi_{u,l}} \in \mathcal{D}$ be the intended PSK information symbol (with $\xi_{u,l}$ the argument of $s_{u,l}$). The signal received at UE u in time-slot l can be written as

$$y_{u,l} = \mathbf{h}_u^{\rm H}\mathbf{x}_l + z_{u,l}, \tag{4}$$

where $\mathbf{x}_l$ denotes the l-th column of $\mathbf{X}$.

To improve the energy efficiency, the idea of CI is exploited. For the PSK modulation, the key of the CI design principle can be captured by the following constraint $(\forall\, u, l)$ [22]

$$\left|\mathrm{Im}(\mathbf{h}_u^{\rm H}\mathbf{x}_l e^{-j\xi_{u,l}})\right| \le \left(\mathrm{Re}(\mathbf{h}_u^{\rm H}\mathbf{x}_l e^{-j\xi_{u,l}}) - \gamma_u\right)\tan(\pi/D),$$

where, as an SNR metric, γ_u measures the quality of received signal. Note that the above CI constraint enforces that the CI pushes received signals away from decision boundaries of the constellation, therefore improving the received SNR without the need to increase the transmit power [22].

Similar to [23], we choose the Cramér-Rao bound (CRB), which measures the performance of an unbiased estimator, as the performance metric of the radar target estimation. For the considered scenario, the CRB of $\mathbf{G}$ is calculated as [23]

$$\mathrm{CRB}(\mathbf{G}) = \sigma_{\rm R}^2 N_{\rm R}/L \cdot \mathrm{tr}\big((\mathbf{X}\mathbf{X}^{\rm H})^{-1}\big). \tag{5}$$

The design goal in this paper is to minimize the CRB subject to the constraints of communication quality and transmit power, which can be formulated as

$$\begin{aligned} \min_{\mathbf{X}} \quad & \mathrm{tr}\big((\mathbf{X}\mathbf{X}^{\rm H})^{-1}\big) \\ \text{s.t.} \quad & \left|\mathrm{Im}(\mathbf{h}_u^{\rm H}\mathbf{x}_l e^{-j\xi_{u,l}})\right| \le \\ & \qquad \big(\mathrm{Re}(\mathbf{h}_u^{\rm H}\mathbf{x}_l e^{-j\xi_{u,l}}) - \gamma_u\big)C_\pi,\ (\forall\, u, l) \\ & \|\mathbf{x}_l\|^2 \le p,\ (\forall\, l), \end{aligned} \tag{6}$$

where p denotes the maximum transmit power for each symbol vector, and $C_\pi = \tan(\pi/D)$ is introduced for simplicity.

Note that problem (6) has a non-convex objective function and consists of a large number of CI constraints, which is challenging to tackle. In particular, the computational complexity of optimizing $\mathbf{X}$ is often prohibitively high, which makes it challenging to implement an algorithm real-time. Moreover, as the size of $\mathbf{X}$ increases (e.g., when L increases), this issue becomes more pronounced. Next, we tackle these issues by designing efficient parallelizable and recursive algorithms.

III. Parallelizable Beamforming Design

In this section, we propose an efficient parallelizable algorithm by exploiting the separability of CI constraints. Apparently, the non-convexity of the objective function of problem (6) prevents efficient solving. To tackle this issue, we choose the first-order approximation method. To this end, we need to derive the (complex) conjugate gradient of $\mathrm{tr}\big((\mathbf{X}\mathbf{X}^{\rm H})^{-1}\big)$. Let $f(\mathbf{X}) = \mathrm{tr}\big((\mathbf{X}\mathbf{X}^{\rm H})^{-1}\big)$. The (complex) conjugate gradient of $f(\mathbf{X})$, denoted by $\partial f/\partial \mathbf{Z}^{\rm H}$, can be calculated as [24]

$$\partial f/\partial \mathbf{Z}^{\rm H} = (\mathbf{X}\mathbf{X}^{\rm H})^{-2}\mathbf{X}. \tag{7}$$

Let $\mathbf{X}_n$ represent the n-th iteration of $\mathbf{X}$. It can be verified that the first-order problem to obtain $\mathbf{X}_{n+1}$ is given by [24]

$$\begin{aligned} \min_{\mathbf{X}} \quad & -\mathrm{Re}\big(\mathrm{tr}((\mathbf{X}_n\mathbf{X}_n^{\rm H})^{-2}\mathbf{X}_n\mathbf{X}^{\rm H})\big) \\ \text{s.t.} \quad & \left|\mathrm{Im}(\mathbf{h}_u^{\rm H}\mathbf{x}_l e^{-j\xi_{u,l}})\right| \le \\ & \qquad \big(\mathrm{Re}(\mathbf{h}_u^{\rm H}\mathbf{x}_l e^{-j\xi_{u,l}}) - \gamma_u\big)C_\pi,\ (\forall\, u, l) \\ & \|\mathbf{x}_l\|^2 \le p,\ (\forall\, l). \end{aligned} \tag{8}$$

To accelerate convergence, a quadratic term is added into the approximate objective function. Let $\rho_n > 0$ denote a penalty parameter. The problem in (8) can be rewritten as

$$\begin{aligned}\min_{\mathbf{X}} \quad & -\operatorname{Re}\big(\operatorname{tr}((\mathbf{X}_n\mathbf{X}_n^{\mathrm{H}})^{-2}\mathbf{X}_n\mathbf{X}^{\mathrm{H}})\big) + \frac{\rho_n}{2}\|\mathbf{X}-\mathbf{X}_n\|_{\mathrm{F}}^2 \\ \text{s.t.} \quad & \big|\operatorname{Im}(\mathbf{h}_u^{\mathrm{H}}\mathbf{x}_l e^{-j\xi_{u,l}})\big| \le \\ & \quad \big(\operatorname{Re}(\mathbf{h}_u^{\mathrm{H}}\mathbf{x}_l e^{-j\xi_{u,l}}) - \gamma_u\big)C_\pi,\ (\forall\, u, l) \\ & \|\mathbf{x}_l\|^2 \le p,\ (\forall\, l).\end{aligned} \tag{9}$$

The rationale for the acceleration is that the objective function becomes strongly convex, which yields better convergence.

Although problem (9) can be solved directly, it can be, in fact, handled more efficiently. For the sake of convenience, we define matrix $\mathbf{C}_n$ and explicitly write $\mathbf{X}_n$ as

$$\begin{aligned}\mathbf{C}_n =&(\mathbf{X}_n\mathbf{X}_n^{\mathrm{H}})^{-2}\mathbf{X}_n = [\mathbf{c}_1, \mathbf{c}_2, \cdots, \mathbf{c}_L] \\ \mathbf{X}_n =&[\mathbf{x}_{1,n}, \mathbf{x}_{2,n}, \cdots, \mathbf{x}_{L,n}].\end{aligned}$$

In view that problem (9) is separable, it is sufficient to solve L independent sub-problems. Specifically, the l-th sub-problem (with respect to $\mathbf{x}_l$) is given by

$$\begin{aligned}\min_{\mathbf{x}_l} \quad & -\operatorname{Re}\big(\mathbf{x}_l^{\mathrm{H}}\mathbf{c}_l\big) + \frac{\rho_n}{2}\|\mathbf{x}_l-\mathbf{x}_{l,n}\|^2 \\ \text{s.t.} \quad & \big|\operatorname{Im}(\mathbf{h}_u^{\mathrm{H}}\mathbf{x}_l e^{-j\xi_{u,l}})\big| \le \\ & \quad \big(\operatorname{Re}(\mathbf{h}_u^{\mathrm{H}}\mathbf{x}_l e^{-j\xi_{u,l}}) - \gamma_u\big)C_\pi,\ (\forall\, u) \\ & \|\mathbf{x}_l\|^2 \le p,\end{aligned} \tag{10}$$

where $\mathbf{x}_l$ denotes the l-th column of matrix $\mathbf{X}$.

Compared to problem (6), whose optimization variable is a matrix, the optimization variable of each problem in (10) is a vector, with much reduced size. Hence, problem (10) can be solved much more efficiently. This advantage becomes more pronounced, as L increases. Moreover, because the separability of CI constraints is exploited, the derived algorithm can be implemented in parallel, which is appealing in practice.

Algorithm 1: Optimization Algorithm for Problem (6)
1: **initialize:** optimization variable $\mathbf{X}_0$ and parameter $\{\rho_n\}$
2: **repeat**
(a) **construct** convex optimization problem (9)
(b) **solve** the constructed optimization problem
3: **until** some convergence criterion is met
4: **output:** (locally optimal) transmit matrix $\mathbf{X}^\star$

Since problem (9) (or (10)) is convex, it can be efficiently solved via a convex optimization toolbox (e.g., CVXOPT or CVXPY). For clarity, the complete iterative procedure is summarized in Algorithm 1. A typical convergence criterion can be $\|\mathbf{X}_n - \mathbf{X}_{n-1}\| \le \varepsilon$, where $\varepsilon > 0$ is a small real number. The iterative algorithm above converges to a stationary point, which is stated in the following theorem.

Theorem 1. *Let $\{\mathbf{X}_n\}$ be a sequence generated by Algorithm 1. Then, every limit point of $\{\mathbf{X}_n\}$ is a stationary point.*

Proof: For the sake of convenience, the feasible set of problem (9) is denoted by $\mathcal{F}$, i.e.,

$$\begin{aligned}\mathcal{F} = \big\{\mathbf{X} \,\big|\, \|\mathbf{x}_l\|^2 \le& p, (\forall\, l), \quad \big|\operatorname{Im}(\mathbf{h}_u^{\mathrm{H}}\mathbf{x}_l e^{-j\xi_{u,l}})\big| \le \\ & \big(\operatorname{Re}(\mathbf{h}_u^{\mathrm{H}}\mathbf{x}_l e^{-j\xi_{u,l}}) - \gamma_u\big)C_\pi, (\forall\, u, l)\big\}.\end{aligned}$$

Then, problem (9) can be equivalently written as

$$\min_{\mathbf{X}} \quad \|\mathbf{X} - \mathbf{X}_n - \mathbf{C}_n/\rho_n\|_{\mathrm{F}}^2 \quad \text{s.t.} \quad \mathbf{X} \in \mathcal{F}. \tag{11}$$

The optimal solution $\mathbf{X}_{n+1}$ of problem (11) can be expressed as $\mathbf{X}_{n+1} = \operatorname{Proj}_{\mathcal{F}}(\mathbf{X}_n + \mathbf{C}_n/\rho_n)$, where $\operatorname{Proj}_{\mathcal{F}}(\cdot)$ denotes the projection of a point onto set $\mathcal{F}$. The convergence of the iteration format above can be obtained by invoking Proposition 2.3.3 in [25]. It is referred to [24] for more details. ■

IV. Recursive Beamforming Design

In the previous algorithm, a matrix variable is optimized each time. In this section, we propose a recursive algorithm, where a vector variable is optimized each time. The key of the recursive method consists of two core operations. The first one is to provide an initial solution, based on which the recursive algorithm can run. The second one is to design an efficient algorithm to optimize $\mathbf{x}_l$ based on $\mathbf{x}_1, \cdots, \mathbf{x}_{l-1}$.

For ease of understanding, we make the following assumption, i.e., each $\mathbf{x}_l$ (transmitted in time-slot l) is optimized in time-slot $l-1$. Let l denote the current time-slot. Then, $\mathbf{X}$ can be decomposed as $\mathbf{X} = [\mathbf{X}_{1:l}, \mathbf{X}_{l+1:}]$, and sub-matrix $\mathbf{X}_{l+1:}$ corresponds to the "future waveform" and "future transmitted information symbols". Hence, up to time-slot l, we only need to consider $\mathbf{X}_{1:l}$, and the problem can be reformulated as

$$\begin{aligned}\min_{\mathbf{X}_{1:l}} \quad & \operatorname{tr}\big((\mathbf{X}_{1:l}\mathbf{X}_{1:l}^{\mathrm{H}})^{-1}\big) \\ \text{s.t.} \quad & \big|\operatorname{Im}(\mathbf{h}_u^{\mathrm{H}}\mathbf{x}_i e^{-j\xi_{u,i}})\big| \le \big(\operatorname{Re}(\mathbf{h}_u^{\mathrm{H}}\mathbf{x}_i e^{-j\xi_{u,i}}) - \gamma_u\big)C_\pi, \\ & \quad (i = 1, \cdots, l, \forall\, u) \\ & \|\mathbf{x}_i\|^2 \le p,\ (i = 1, \cdots, l).\end{aligned}$$

As a recursive algorithm, when optimizing $\mathbf{X}_{1:l}$, sub-matrix $\mathbf{X}_{1:l-1}$ has already been available. Hence, in time-slot $l-1$, the task is to optimize vector $\mathbf{x}_l$ given sub-matrix $\mathbf{X}_{1:l-1}$, i.e.,

$$\begin{aligned}\min_{\mathbf{x}_l} \quad & \operatorname{tr}\big((\mathbf{X}_{1:l}\mathbf{X}_{1:l}^{\mathrm{H}})^{-1}\big) \\ \text{s.t.} \quad & \big|\operatorname{Im}(\mathbf{h}_u^{\mathrm{H}}\mathbf{x}_l e^{-j\xi_{u,l}})\big| \le \\ & \quad \big(\operatorname{Re}(\mathbf{h}_u^{\mathrm{H}}\mathbf{x}_l e^{-j\xi_{u,l}}) - \gamma_u\big)C_\pi,\ (\forall\, u) \\ & \|\mathbf{x}_l\|^2 \le p.\end{aligned} \tag{12}$$

By leveraging the well-known matrix inversion lemma, the objective function in problem (12) can be expressed as

$$\begin{aligned}&\big(\mathbf{X}_{1:l}\mathbf{X}_{1:l}^{\mathrm{H}}\big)^{-1} = \big(\mathbf{X}_{1:l-1}\mathbf{X}_{1:l-1}^{\mathrm{H}} + \mathbf{x}_l\mathbf{x}_l^{\mathrm{H}}\big)^{-1} \\ =&\big(\mathbf{X}_{1:l-1}\mathbf{X}_{1:l-1}^{\mathrm{H}}\big)^{-1} - \\ &\quad \frac{\big(\mathbf{X}_{1:l-1}\mathbf{X}_{1:l-1}^{\mathrm{H}}\big)^{-1}\mathbf{x}_l\mathbf{x}_l^{\mathrm{H}}\big(\mathbf{X}_{1:l-1}\mathbf{X}_{1:l-1}^{\mathrm{H}}\big)^{-1}}{1 + \mathbf{x}_l^{\mathrm{H}}\big(\mathbf{X}_{1:l-1}\mathbf{X}_{1:l-1}^{\mathrm{H}}\big)^{-1}\mathbf{x}_l}.\end{aligned}$$

Let $\mathbf{A}_{l-1} = \big(\mathbf{X}_{1:l-1}\mathbf{X}_{1:l-1}^{\mathrm{H}}\big)^{-1}$. The optimization problem in (12) can be equivalently written as

$$\begin{aligned}\max_{\mathbf{x}_l} \quad & \operatorname{tr}\left(\frac{\mathbf{A}_{l-1}\mathbf{x}_l\mathbf{x}_l^{\mathrm{H}}\mathbf{A}_{l-1}}{1 + \mathbf{x}_l^{\mathrm{H}}\mathbf{A}_{l-1}\mathbf{x}_l}\right) = \frac{\mathbf{x}_l^{\mathrm{H}}\mathbf{A}_{l-1}^2\mathbf{x}_l}{1 + \mathbf{x}_l^{\mathrm{H}}\mathbf{A}_{l-1}\mathbf{x}_l} \\ \text{s.t.} \quad & \big|\operatorname{Im}(\mathbf{h}_u^{\mathrm{H}}\mathbf{x}_l e^{-j\xi_{u,l}})\big| \le \\ & \quad \big(\operatorname{Re}(\mathbf{h}_u^{\mathrm{H}}\mathbf{x}_l e^{-j\xi_{u,l}}) - \gamma_u\big)C_\pi,\ (\forall\, u) \\ & \|\mathbf{x}_l\|^2 \le p.\end{aligned} \tag{13}$$

Remark 4.1 Compared to problem (6), whose optimization variable is a matrix, the optimization variable of problem (13) is only a vector. Moreover, the number of constraints in (13) is about $1/L$ of that of problem (6). As a result, the complexity of problem (13) is much lower than that of problem (6).

Although problem (13) involves only a vector optimization variable $\mathbf{x}_l$, it cannot be solved directly. Next, we propose an efficient algorithm to address this problem. By introducing a variable t, problem (13) can be equivalently written as

$$\begin{aligned} \max_{\mathbf{x}_l, t} \quad & t \\ \text{s.t.} \quad & t^{-1}\mathbf{x}_l^{\mathrm{H}}\mathbf{A}_{l-1}^2\mathbf{x}_l \geq 1 + \mathbf{x}_l^{\mathrm{H}}\mathbf{A}_{l-1}\mathbf{x}_l \\ & \left|\mathrm{Im}(\mathbf{h}_u^{\mathrm{H}}\mathbf{x}_l e^{-j\xi_{u,l}})\right| \leq \\ & \qquad \left(\mathrm{Re}(\mathbf{h}_u^{\mathrm{H}}\mathbf{x}_l e^{-j\xi_{u,l}}) - \gamma_u\right)C_\pi, \ (\forall\, u) \\ & \|\mathbf{x}_l\|^2 \leq p. \end{aligned} \tag{14}$$

The successive convex approximation (SCA) technique can be used to solve problem (14). Let $\mathbf{x}_{l,n}$ and t_n denote the n-th iterations of $\mathbf{x}_l$ and t, respectively. The $(n+1)$-th iterations can be obtained by solving the following convex problem

$$\begin{aligned} \max_{\mathbf{x}_l, t} \quad & t \\ \text{s.t.} \quad & \frac{2\mathrm{Re}\left(\mathbf{x}_{l,n}^{\mathrm{H}}\mathbf{A}_{l-1}^2\mathbf{x}_l\right)}{t_n} - \frac{\mathbf{x}_{l,n}^{\mathrm{H}}\mathbf{A}_{l-1}^2\mathbf{x}_{l,n}}{t_n^2}t \\ & \qquad \geq 1 + \mathbf{x}_l^{\mathrm{H}}\mathbf{A}_{l-1}\mathbf{x}_l \\ & \left|\mathrm{Im}(\mathbf{h}_u^{\mathrm{H}}\mathbf{x}_l e^{-j\xi_{u,l}})\right| \leq \\ & \qquad \left(\mathrm{Re}(\mathbf{h}_u^{\mathrm{H}}\mathbf{x}_l e^{-j\xi_{u,l}}) - \gamma_u\right)C_\pi, \ (\forall\, u) \\ & \|\mathbf{x}_l\|^2 \leq p. \end{aligned} \tag{15}$$

The iterative procedure to solve problem (13) is summarized in Algorithm 2, which also converges to a stationary point.

Algorithm 2: Iterative Algorithm for Problem (13) or (14)

1: **initialize:** optimization variables $\mathbf{x}_{l,0}$ and t_0; let $n = 0$
2: **repeat**
 (a) **construct** convex optimization problem (15)
 (b) **solve** constructed problem to update $\mathbf{x}_l \Rightarrow \mathbf{x}_{l,n+1}$
 (c) **check** convergence criterion and let $n \leftarrow n + 1$
3: **until** some convergence criterion is met
4: **output:** optimal solution $\mathbf{x}_l^\star$

For completeness, the complete recursive procedure for one communication frame is provided in Algorithm 3. To start the recursive algorithm, an initial solution (e.g., a sub-matrix of $\mathbf{X}$) is required, which can be obtained by solving

$$\begin{aligned} \min_{\mathbf{X}\in\mathbb{C}^{N_{\mathrm{T}}\times K}} \quad & \mathrm{tr}\left((\mathbf{X}\mathbf{X}^{\mathrm{H}})^{-1}\right) \\ \text{s.t.} \quad & \left|\mathrm{Im}(\mathbf{h}_u^{\mathrm{H}}\mathbf{x}_l e^{-j\xi_{u,l}})\right| \leq \left(\mathrm{Re}(\mathbf{h}_u^{\mathrm{H}}\mathbf{x}_l e^{-j\xi_{u,l}}) - \gamma_u\right)C_\pi, \\ & \qquad (l = 1, \cdots, K, \forall\, u) \\ & \|\mathbf{x}_l\|^2 \leq p, \ (l = 1, \cdots, K). \end{aligned}$$

Since the size of $\mathbf{X}$ above is $N_{\mathrm{T}} \times K$ with $N_{\mathrm{T}} \leq K \ll L$, the complexity of solving the problem above is small.

Finally, we highlight an important property of the proposed recursive algorithm, i.e., the monotonicity in terms of recursive procedure, which is stated in the following theorem.

Algorithm 3: Recursive Beamforming Procedure ($L \gg N_{\mathrm{T}}$)

1: **input:** K - dimension of initial sub-matrix; $\{\mathbf{h}_u\}$ - CSI
2: **initialize:**
 (a) **find** an initial sub-matrix $\mathbf{X}_{1:K}$ and compute $\mathbf{A}_K$
 (b) **set** counter $n \leftarrow K$
3: **repeat**
 (a) **construct** optimization problem (13) with $l = n + 1$
 (b) **solve** constructed problem via Algorithm 2 $\Rightarrow$ precoded signal vector $\mathbf{x}_l^\star$ for time-slot l
 (c) **update** counter $n \leftarrow n + 1$
 until $n \geq L$

Theorem 2. *Under the assumption that the problem used to obtain the initial solution is feasible, the recursive algorithm strictly monotonously decreases the objective function value as the recursive procedure proceeds (or index l increases).*

Proof: See Appendix A. ∎

Theorem 2 shows that the proposed recursive algorithm will not degenerate system performance. Hence, the oscillation or degeneration phenomenon (typically, due to iterations) existing widely in many algorithms will not occur in our algorithm.

V. Simulation Results

In this section, simulation results are provided to demonstrate the performance of the proposed algorithms. The distribution of receiving noise of either radar or communication is fixed to $\mathcal{CN}(\mathbf{0}, \mathbf{I})$. Similar to [23], the channel vector of each UE u is distributed as $\mathbf{h}_u \sim \mathcal{CN}(\mathbf{0}, \mathbf{I})$, and the uniform linear array is considered here. The mean square error (MSE) [1] and symbol error rate (SER) are chosen as the performance metrics. We compare our algorithms against the most relevant benchmark in [23], in which the CRB is similarly minimized but subject to the classical block-level precoding (BLP) mode. For the sake of convenience, the parallelizable algorithm (i.e., Algorithm 1) and recursive algorithm (i.e., Algorithm 3) are named as Paral-SLP and Recur-SLP, respectively.

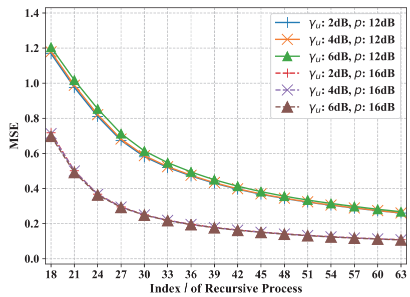

Fig. 1. The monotonicity of the recursive beamforming design (Algorithm 3): $U = 6$, $L = 64$, $N_{\mathrm{T}} = 16$ and $N_{\mathrm{R}} = 20$.

First, we confirm the monotonicity of the proposed recursive algorithm. It is seen from Fig. 1 that as the recursive process

[1] Similar to [23], we exclusively consider the case that the entries of the target response matrix $\mathbf{G}$ in (3) are independently and identically distributed as $\mathcal{CN}(0, 1)$. It corresponds to a Swerling 1 or Swerling 2 target with Gaussian distributed complex amplitude. In this case, the CRB is equal to the MSE.

proceeds (i.e., l increases), the MSE decreases monotonously and strictly, which coincides with our theoretical analysis. It is also observed that the MSE decreases fast at the beginning part of the recursive process (e.g., when l varies from 18 to 36), which implies that good radar sensing performance can be achieved even with a small amount of resources.

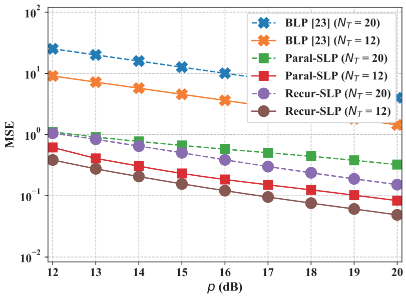

Fig. 2. Target estimation MSE of different beamforming algorithms: $U = 4$, $L = 32$, $N_{\mathrm{R}} = 24$ and $\gamma_u = 8$dB.

Next, we evaluate different beamforming algorithms from the perspective of MSE and SER. The target estimation MSE of different algorithms is shown in Fig. 2. Since the CI-based SLP can exploit the interference, it is not surprising that the SLP algorithms outperform the BLP counterpart. Interestingly, we can observe that the recursive algorithm is superior to the non-recursive counterpart. In fact, since the objective function of the optimization problem considered is highly nonlinear and non-convex, it is difficult (and even impossible) to find the globally optimal solution. The monotonicity of the recursive algorithm guarantees to improve the performance of interest continuously, which alleviates possible unpredictable influence due to the non-convexity of the optimization problem.

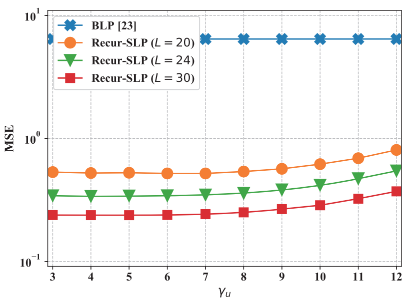

Fig. 3. Target estimation MSE of different beamforming algorithms (varying with γ_u): $U = 4$, $N_{\mathrm{T}} = 16$, $N_{\mathrm{R}} = 24$ and $p = 16$dB.

The performance tradeoff between radar sensing and communication is shown in Fig. 3. The CRB for target estimation becomes higher, as the SNR threshold of the UEs increases. Equivalently, as the quality of communication becomes better, the radar sensing performance decreases. Note, however, that although the CRB of the SLP algorithm becomes larger as the SNR increases, it still remains at a low level, which clearly shows the advantage of the SLP-based design mode.

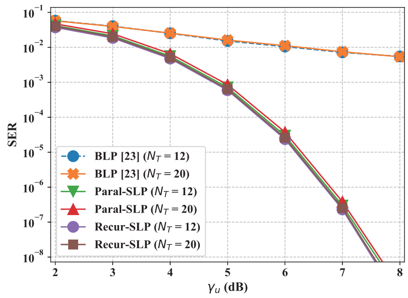

Fig. 4. The SER of different beamforming algorithms: $U = 4$, $L = 32$, $N_{\mathrm{R}} = 24$ and $p = 15$dB.

The SER performance of different algorithms is shown in Fig. 4. It can be observed that the SER performance achieved by the SLP-based algorithms is much better than that of the BLP counterpart. The reason for this is that the CI constraints enforce that the distance between the received signals and the decision boundaries is no less than the predefined value, which guarantees a stable SER performance, e.g., the SER achieved declines exponentially with respect to the SNR.

VI. Conclusion

In this paper, we incorporated CI-based SLP mode into the design of joint radar sensing and communication beamforming. First, we proposed a highly parallelizable algorithm to reduce the computational complexity. Then, we proposed the idea of recursive design as well as an efficient algorithm. We confirmed the advantages of our proposal via experiments.

Appendix A
Proof of Theorem 2

We shall use induction to prove this theorem. Let n denote the induction index, taking values $K, K+1, K+2, \cdots$.

Step 1. For $n = K$, the optimization problem used to find out an initial solution is given by

$$\begin{aligned}
\min_{\mathbf{X}\in\mathbb{C}^{U\times K}} \quad & \mathrm{tr}\big((\mathbf{X}\mathbf{X}^{\mathrm{H}})^{-1}\big) \\
\text{s.t.} \quad & \big|\mathrm{Im}(\mathbf{h}_u^{\mathrm{H}}\mathbf{x}_l e^{-j\xi_{u,l}})\big| \leq \big(\mathrm{Re}(\mathbf{h}_u^{\mathrm{H}}\mathbf{x}_l e^{-j\xi_{u,l}}) - \gamma_u\big) C_\pi, \\
& \quad (l = 1, \cdots, K, \forall\, u) \\
& \|\mathbf{x}_l\|^2 \leq p,\ (l = 1, \cdots, K).
\end{aligned} \tag{16}$$

According to the assumption of the theorem (i.e., problem (16) is feasible), a solution of the problem, denoted by $\mathbf{X}_K$, satisfies $\mathrm{tr}\big((\mathbf{X}_K\mathbf{X}_K^{\mathrm{H}})^{-1}\big) < \infty$. Combining the fact $\mathbf{X}_K\mathbf{X}_K^{\mathrm{H}} \succeq \mathbf{0}$, we can assert that $\mathbf{X}_K\mathbf{X}_K^{\mathrm{H}} \succ \mathbf{0}$ holds. Hence, $\mathbf{A}_K = (\mathbf{X}_K\mathbf{X}_K^{\mathrm{H}})^{-1}$ is also strictly positive definite, i.e., $\mathbf{A}_K \succ \mathbf{0}$.

To seek the solution for $n = K+1$, the recursive procedure solves the following optimization problem

$$\begin{aligned}\max_{\mathbf{x}_l} \quad & \frac{\mathbf{x}_l^{\mathrm{H}}\mathbf{A}_K^2\mathbf{x}_l}{1+\mathbf{x}_l^{\mathrm{H}}\mathbf{A}_K\mathbf{x}_l} \\ \text{s.t.} \quad & \left|\mathrm{Im}(\mathbf{h}_u^{\mathrm{H}}\mathbf{x}_l e^{-j\xi_{u,l}})\right| \leq \\ & \quad \left(\mathrm{Re}(\mathbf{h}_u^{\mathrm{H}}\mathbf{x}_l e^{-j\xi_{u,l}}) - \gamma_u\right)C_\pi, \, (\forall\, u) \\ & \|\mathbf{x}_l\|^2 \leq p. \end{aligned} \tag{17}$$

Since the set of constraints of problem (17) is a proper subset of that of problem (16) and the objective function of problem (17) is well-defined for the entire space $\mathbb{C}^{N_{\mathrm{T}}}$, the feasibility of problem (17) indicates that the feasible set of problem (17), denoted by $\mathcal{F}_l$, is nonempty. Note that $\mathbf{0} \notin \mathcal{F}_l$ holds. Otherwise, the CI constraints violate.

The solution of problem (17) is denoted by $\mathbf{x}_{K+1}$. Since $\mathbf{A}_K \succ \mathbf{0}$ and $\mathbf{x}_{K+1}\mathbf{x}_{K+1}^{\mathrm{H}} \succeq \mathbf{0}$ hold, we can obtain

$$\begin{aligned}\mathbf{A}_{K+1}^{-1} =& \mathbf{X}_K\mathbf{X}_K^{\mathrm{H}} + \mathbf{x}_{K+1}\mathbf{x}_{K+1}^{\mathrm{H}} \\ =& \mathbf{A}_K^{-1} + \mathbf{x}_{K+1}\mathbf{x}_{K+1}^{\mathrm{H}} \succ \mathbf{0}.\end{aligned}$$

Hence, $\mathbf{A}_{K+1} \succ \mathbf{0}$ holds. Note that the two facts $\mathbf{A}_K \succ \mathbf{0}$ and $\mathbf{x}_{K+1} \neq 0$ imply that $\mathbf{x}_{K+1}^{\mathrm{H}}\mathbf{A}_K^2\mathbf{x}_{K+1} > 0$ holds, i.e., the objective function must strictly decrease. The above discussion shows that the theorem holds true for $n = K$.

Step 2. It is sufficient to show that the theorem holds as well for $n = N+1$ if it holds for $n = N > K$. Note that the required induction procedure is similar to that in Step 1, which is omitted to avoid repetition. In view of the above discussion and using induction, we have proven the theorem.

APPENDIX B
ACKNOWLEDGMENTS

This work was supported by the National Natural Science Foundation of China under Grants 62301249, 61720106003 and 62225107, the Shenzhen Science and Technology Program under Grant 20220815100308002, the Foundation Research Project of Jiangsu Province under Grant BK20230878, the Young Elite Scientist Sponsorship Program by the China Association for Science and Technology (CAST) under Grant No. YESS20210055, and the Engineering and Physical Sciences Research Council, UK under project EP/S028455/1.

REFERENCES

[1] F. Liu, Y. Cui, C. Masouros, J. Xu, T. X. Han, Y. C. Eldar, and S. Buzzi, "Integrated sensing and communications: Towards dual-functional wireless networks for 6G and beyond," *IEEE J. Sel. Areas Commun.*, pp. 1–1, 2022.

[2] F. Liu, C. Masouros, A. P. Petropulu, H. Griffiths, and L. Hanzo, "Joint radar and communication design: Applications, state-of-the-art, and the road ahead," *IEEE Trans. Commun.*, vol. 68, no. 6, pp. 3834–3862, 2020.

[3] A. Hassanien, M. G. Amin, E. Aboutanios, and B. Himed, "Dual-function radar communication systems: A solution to the spectrum congestion problem," *IEEE Signal Process. Mag.*, vol. 36, no. 5, pp. 115–126, 2019.

[4] K. Wu, J. A. Zhang, X. Huang, Y. J. Guo, and R. W. Heath, "Waveform design and accurate channel estimation for frequency-hopping MIMO radar-based communications," *IEEE Trans. Commun.*, vol. 69, no. 2, pp. 1244–1258, 2021.

[5] T. Huang, N. Shlezinger, X. Xu, Y. Liu, and Y. C. Eldar, "MAJoRCom: A dual-function radar communication system using index modulation," *IEEE Trans. Signal Process.*, vol. 68, pp. 3423–3438, 2020.

[6] A. Zhang, M. L. Rahman, X. Huang, Y. J. Guo, S. Chen, and R. W. Heath, "Perceptive mobile networks: Cellular networks with radio vision via joint communication and radar sensing," *IEEE Veh. Technol. Mag.*, vol. 16, no. 2, pp. 20–30, 2021.

[7] A. Ali, N. Gonzalez-Prelcic, R. W. Heath, and A. Ghosh, "Leveraging sensing at the infrastructure for mmWave communication," *IEEE Commun. Mag.*, vol. 58, no. 7, pp. 84–89, 2020.

[8] P. Kumari, S. A. Vorobyov, and R. W. Heath, "Adaptive virtual waveform design for millimeter-wave joint communicationcradar," *IEEE Trans. Signal Process.*, vol. 68, pp. 715–730, 2020.

[9] F. Liu, C. Masouros, A. Li, H. Sun, and L. Hanzo, "MU-MIMO communications with MIMO radar: From co-existence to joint transmission," *IEEE Trans. Wireless Commun.*, vol. 17, no. 4, pp. 2755–2770, 2018.

[10] F. Liu, L. Zhou, C. Masouros, A. Li, W. Luo, and A. Petropulu, "Toward dual-functional radar-communication systems: Optimal waveform design," *IEEE Trans. Signal Process.*, vol. 66, no. 16, pp. 4264–4279, 2018.

[11] X. Liu, T. Huang, N. Shlezinger, Y. Liu, J. Zhou, and Y. C. Eldar, "Joint transmit beamforming for multiuser MIMO communications and MIMO radar," *IEEE Trans. Signal Process.*, vol. 68, pp. 3929–3944, 2020.

[12] X. Yuan, Z. Feng, J. A. Zhang, W. Ni, R. P. Liu, Z. Wei, and C. Xu, "Spatio-temporal power optimization for MIMO joint communication and radio sensing systems with training overhead," *IEEE Trans. Veh. Technol.*, vol. 70, no. 1, pp. 514–528, 2021.

[13] Y. Liu, G. Liao, J. Xu, Z. Yang, and Y. Zhang, "Adaptive OFDM integrated radar and communications waveform design based on information theory," *IEEE Commun. Lett.*, vol. 21, no. 10, pp. 2174–2177, 2017.

[14] Y. Cui, F. Liu, X. Jing, and J. Mu, "Integrating sensing and communications for ubiquitous IoT: Applications, trends, and challenges," *IEEE Netw.*, vol. 35, no. 5, pp. 158–167, 2021.

[15] A. Li, F. Liu, C. Masouros, Y. Li, and B. Vucetic, "Interference exploitation 1-bit massive mimo precoding: A partial branch-and-bound solution with near-optimal performance," *IEEE Trans. Wireless Commun.*, vol. 19, no. 5, pp. 3474–3489, 2020.

[16] C. Masouros, M. Sellathurai, and T. Ratnarajah, "Vector perturbation based on symbol scaling for limited feedback MISO downlinks," *IEEE Trans. Signal Process.*, vol. 62, no. 3, pp. 562–571, 2014.

[17] C. Masouros and E. Alsusa, "Dynamic linear precoding for the exploitation of known interference in MIMO broadcast systems," *IEEE Trans. Wireless Commun.*, vol. 8, no. 3, pp. 1396–1404, 2009.

[18] C. Masouros, "Correlation rotation linear precoding for MIMO broadcast communications," *IEEE Trans. Signal Process.*, vol. 59, no. 1, pp. 252–262, 2011.

[19] C. Masouros and T. Ratnarajah, "Interference as a source of green signal power in cognitive relay assisted co-existing MIMO wireless transmissions," *IEEE Trans. Commun.*, vol. 60, no. 2, pp. 525–536, 2012.

[20] F. Liu, C. Masouros, A. Li, T. Ratnarajah, and J. Zhou, "MIMO radar and cellular coexistence: A power-efficient approach enabled by interference exploitation," *IEEE Trans. Signal Process.*, vol. 66, no. 14, pp. 3681–3695, 2018.

[21] R. Liu, M. Li, Q. Liu, and A. L. Swindlehurst, "Dual-functional radar-communication waveform design: A symbol-level precoding approach," *IEEE J. Sel. Topics Signal Process.*, vol. 15, no. 6, pp. 1316–1331, 2021.

[22] C. Masouros and G. Zheng, "Exploiting known interference as green signal power for downlink beamforming optimization," *IEEE Trans. Signal Process.*, vol. 63, no. 14, pp. 3628–3640, 2015.

[23] F. Liu, Y.-F. Liu, A. Li, C. Masouros, and Y. C. Eldar, "Cramer-Rao bound optimization for joint radar-communication beamforming," *IEEE Trans. Signal Process.*, vol. 70, pp. 240–253, 2022.

[24] J. Zhang, C. Masouros, F. Liu, and Y. Huang, "Low-complexity joint radar-communication beamforming: From optimization to deep unfolding," *Submitted to IEEE Trans. Signal Process.*, 2023.

[25] D. P. Bertsekas, *Nonlinear Programming*, 2nd ed. Athena Scientific, 1999.